Histol Histopathol (2020) 35: 289-301

**http://www.hh.um.es**

**Histology and Histopathology**

*From Cell Biology to Tissue Engineering*

# Adipose-derived stem cells and adipose-derived stem cell-conditioned medium modulate *in situ* imbalance between collagen I- and collagen V-mediated IL-17 immune response recovering bleomycin pulmonary fibrosis

**Renato Gonçalves Felix[1], Ana Livia Carvalho Bovolato[1], Ondina Silvia Cotrim[1], Patricia dos Santos Leão[2], Sabrina Setembre Batah[2], Márjorie de Assis Golim[1], Ana Paula Velosa[3], Walcy Teodoro[3], Vanessa Martins[4], Fernanda Ferreira Cruz[5], Elenice Deffune[1], Alexandre Todorovic Fabro[2] and Vera Luiza Capelozzi[4]**

[1]Botucatu Medical School, São Paulo State University, [2]Department of Pathology, Ribeirão Preto Medical School, [3]Rheumatology Division, [4]Department of Pathology, Faculty of Medicine, University of São Paulo, São Paulo and [5]Laboratory of Pulmonary Investigation, Institute of Biophysics Carlos Chagas Filho, Federal University of Rio de Janeiro, Brazil

**Summary.** The immunogenic collagen V (Col V) and the proinflammatory cytokine interleukin (IL)-17 have been implicated in the pathogenesis of multiple autoimmune diseases. Col V is also up-regulated during adipogenesis and can stimulate adipocyte differentiation *in vitro*. Conditioned medium (CM) generated from adipose-derived mesenchymal stem cells (MSCs) reduces bleomycin (BLM)-induced lung injury in rats, suggesting a crucial role *in situ* of immunomodulatory factors secreted by MSCs in these beneficial effects. In the present work, we investigated this hypothesis, analyzing levels of plasma inflammatory mediators and inflammatory and fibrotic mediators in the lung tissue of BLM-injured rats after treatment with MSCs and CM. Pulmonary fibrosis was intratracheally induced by BLM. After 10 days, BLM animals were further randomized into subgroups receiving saline, MSCs, or CM intravenously. On days 14 and 21, the animals were euthanized, and the lungs were examined through protein expression of nitric oxide synthase (NOS), IL-17, transforming growth factor-β (TGF-β), vascular endothelial growth factor, endothelin-1, and the immunogenic Col V through histological quantitative evaluation and plasma levels of fibrinogen, Von Willebrand factor, and platelet-derived growth factor (PDGF). Rats that had been injected with MSCs and CM showed a significant increase in weight and significant improvements at 14 and 21 days after intravenous injection at both time points of analysis of plasma fibrinogen, PDGF, and Von Willebrand factor and NOS-2 expression, supporting an early anti-inflammatory action, thus reducing TGF-β and collagen I fibers. In contrast, intravenous injection of CM was able to significantly increase the deposition of Col V fibers and IL-17 on both day 14 and day 21 as compared with the amount observed in rats from the BLM group and MSC groups. In conclusion, this study reinforces previous observations on the therapeutic properties of MSCs and CM and is the first report to demonstrate the association of its actions with immunomodulatory biomarkers on lung tissue. We concluded that adipose-derived stem cells and adipose-derived stem cells-CM modulate an *in situ* imbalance between collagen I- and Col V-mediated IL-17 immune response, emerging as a promising therapeutic option for recovering from BLM pulmonary fibrosis.

**Key words:** Adipose-derived mesenchymal stem cells, Conditioned medium, Collagen fibers, Growth factors, Cytokines, IL-17, Bleomycin, Collagen V, Electron microscopy

*Offprint requests to:* Prof Vera Luiza Capelozzi, Department of Pathology, Faculdade de Medicina da Universidade de São Paulo, Av. Dr. Arnaldo 455, sala 1143, Zip code 01246-903, São Paulo, SP, Brazil. e-mail: vera.capelozzi@fm.usp.br

DOI: 10.14670/HH-18-152

## Introduction

Type V collagen (Col V) is a minor collagen found primarily within the fibrils of the major lung collagen, type I and type III. Col V regulates collagen fiber assembly, geometry, and strength and links stromal collagen to the basement membrane (Sun et al., 2011; Wenstrup et al., 2011). Lung injury may lead to the exposure of this normally sequestered antigen, rendering it available for activation of an autoimmune response (Weber and Wilkes, 2013). A sustained autoimmune response may lead to abnormal lung remodeling, as evidenced in clinical and preclinical studies showing that increased levels of Col V correlate with fibrosis and disease progression (Parra et al., 2006; Vittal et al., 2013a,b; Lei et al., 2016). The proinflammatory cytokine interleukin (IL)-17 has also been implicated in the pathogenesis of multiple autoimmune diseases (Axtell et al., 2010; Nakano et al., 2011). Transforming growth factor-β (TGF-β) is a strong inducer of IL-17 (Mangan et al., 2006), and IL-17, in turn, may be involved in lung fibrogenesis in TGF-β-dependent and -independent pathways (Mi et al., 2011). Vittal and colleagues (Vittal et al., 2013a) reported in murine orthotopic lung transplants a feed-forward loop between IL-17 and TGF-β, leading to induction of Col V and associated epithelial repair in lung fibrosis. Fabro and colleagues (Fabro et al., 2015) showed that IL-17 interacts with expression of Col V in the late state of experimental pulmonary fibrosis. Vascular endothelial growth factor (VEGF) modulates extracellular matrix (ECM) synthesis and composition by regulating the Col V gene (Yang et al., 2018). In turn, ECM provides a supportive microenvironment for adipose tissue growth and function (Mariman and Wang, 2010). Col V is up-regulated during adipogenesis and can stimulate adipocyte differentiation *in vitro* (Nakajima et al., 2002a, b). However, the immunomodulatory role of Col V during *in vivo* adipose tissue growth is unknown.

The immunomodulatory functions of mesenchymal stem cells (MSCs) have recently caused enthusiasm for researchers examining their potential therapeutic application in a variety of immune disorder diseases (Shi et al., 2010). MSCs have been tested in rodent models to treat diseases in which immunodysregulation is thought to be the main pathogenic mechanism. It has been shown that MSCs can reverse autoimmune response disorder by modulating multiple subsets of immune cells (Gerdoni et al., 2007). In addition, their pluripotent nature may also benefit idiopathic pulmonary fibrosis patients by directly or indirectly promoting alveolar repair (Weiss et al., 2011). Recent studies have demonstrated the capability of MSCs to inhibit bleomycin (BLM)-induced pneumonitis and fibrosis in a mouse model (Murphy et al., 2011). However, there are restrictions to the extensive clinical application because of the necessity for invasive procedures to isolate and process cells. Adipose-derived MSCs are adult cells that possess the capacity for homing, immunomodulation, promotion of repair, and direct regeneration of damaged tissues, which make them promising therapeutic candidates (Bateman et al., 2018). Moreover, MSCs can be easily obtained in profusion from subcutaneous tissue. Regardless of the obvious useful effects of adipose MSCs on lung fibrosis, there have been no clear reports on the mechanism through which these cells act. The statement that cell treatment effectiveness has also been observed in the absence of significant levels of adipose-derived cell engraftment (Reddy et al., 2016) suggests that these cells could act through the paracrine mechanism associated with extracellular vesicles and much less due to releasing soluble factors. The microvesicles and exosomes are capable of exerting repair actions on lung parenchyma recruiting inflammatory cells to the injury site. Nevertheless, important questions persist concerning the positive properties exerted by conditioned medium (CM) on pulmonary fibrosis and whether these properties are specific to CM or if they are instead also exerted by MSCs. Therefore, the identification of factors that regulate adipose tissue morphology could lead to new therapies to treat fibrotic diseases.

In the present study, using the murine model of BLM-induced lung fibrosis described previously (Srour and Thebaud, 2015; Reddy et al., 2016), we explored some of the properties of CM in reducing the severity and progression of lung fibrosis *in vivo*. Furthermore, to better understand the immunomodulatory mechanism that may support the positive effects of CM, we also quantified the levels of plasma inflammatory mediators (fibrinogen, Von Willebrand factor, and platelet-derived growth factor [PDGF]), inflammatory and fibrotic mediators (nitric oxide synthase [NOS], IL-17, TGF-β, VEGF, endothelin-1) and the immunogenic Col V in the lung tissue of BLM-injured rats after treatment with CMs. For all of these experiments, we compared the effects of CMs with MSCs.

## Materials and methods

### *Ethics statements*

This study was approved by the Institutional Animal Care and Use Committee of the Health Sciences Centre, Botucatu Medical School, São Paulo State University, under protocol No. 530/13 of 02.06.2014. All animals received humane care in compliance with the "Principles of Laboratory Animal Care" formulated by the National Society for Medical Research and the US National Academy of Sciences Guide for the Care and Use of Laboratory Animals. The present study followed the ARRIVE guidelines for reporting of animal research (Kilkenny et al., 2010).

### *Cells used to prepare CMs*

CMs were generated from the culture of the adipose mesenchymal tissue cells isolated from the interscapular

region, from five animal donors, following a well-established protocol of our laboratory (Bertanha et al., 2014). As previously described (Moroz et al., 2013), following the third cell culture passage, cells were characterized using specific antibodies designed for flow cytometry. Anti-CD90 antibody (clone OX-7, cross-reactivity with rabbit; Biolegend) was used as a positive marker for MSCs. Anti-CD34 and anti-CD45 antibodies (Biolegend, San Diego, Calif) were employed as negative markers. Anti-mouse-IgG conjugated with fluorescein isothiocyanate was used as the secondary antibody (Molecular Probes, Eugene, Ore). Further analysis was conducted with the FacsCalibur (BD Biosciences, San Jose, Calif) equipment and software to obtain the number of positive CD90 cells. In addition, the obtained MSCs were investigated for their potential to differentiate into the osteogenic, chondrogenic, and adipogenic lineages, under the recommended differentiation cell culture media (StemPro adipogenesis, chondrogenesis, and osteogenesis kits; Invitrogen) (data not shown).

### *Adipose tissue-derived MSC culture and CM preparation*

CMs were generated from *in vitro* cultures of adipose MSCs. Adipose tissue-derived MSCs were obtained as previously described (de Mattos Carvalho et al., 2009) through digestion reaction with type I collagenase (Invitrogen). Cell culture procedures started with $2\times10^4$ cells/cm$^2$ seeding and expansion in six-well culture plates (Techno Plastic Products, Trasadingen, Switzerland) with Dulbecco's modified Eagle's medium nutrient F12 mixture medium, supplemented with 10% fetal bovine serum, 100 U/mL penicillin, 100 mg/mL streptomycin, 25 mg/mL amphotericin B (2 mmol/L L-glutamine; Invitrogen), 1% (v/v) minimum essential medium (MEM) essential amino acids solution (×50; Invitrogen), and 0.5% (v/v) of 10 mM MEM nonessential amino acids solution (×100; Invitrogen) until reaching 80% confluence, when the obtained monolayers were detached from culture wells with 0.25% trypsin/ethylenediamine-tetraacetic acid (Invitrogen) and seeded in 75-cm$^2$ culture flasks (Nunc, Roskilde, Denmark). When MSCs at third or higher passages reached between 70% and 80% confluence, the medium was discarded and cells were rinsed three times with phosphate-buffered saline (PBS). Cells were then cultured with serum-free medium for 24 hours. The CMs were collected and filtered through a 0.2-μm filter to remove cellular debris. Adherent cells were trypsinized, stained with trypan blue, and counted. The media from $1\times10^6$ cells yielded 15 mL of primary CMs that were further concentrated approximately 25-fold (i.e., 200 μL CM) using ultrafiltration units with a 3-kDa molecular weight cutoff (Amicon Ultra-PL 3; EMD Millipore Corporation, Billerica, MA, http://www.emdmillipore.com). Concentrated CM (200 μL) collected from the same amount of administered cells ($1\times10^6$ cells) was injected in the rats (Ionescu et al., 2012a,b; Cruz et al., 2015).

### *Induction of lung injury in rats*

All experimental procedures were performed on anesthetized animals (by intramuscular injection of 10 mg/kg intraperitoneal ketamine from Park-Davis and 0.3 mg/kg xylazine from Rompum, Bayer, Brazil), and all efforts were made to minimize animal suffering. A total of 40 Wistar rats, aged 8 weeks old, from the CEMIB Multidisciplinary Center for Biological Research of Unicamp University were used. Among these, 30 were instilled intratracheally with BLM (1.5U in 0.05 mL of saline, single dose, equivalent to 1.5 mg/kg) as previously described (Kim et al., 2010; Fabro et al., 2015), whereas the remaining 10 were instilled intratracheally with 0.05 mL saline, thus representing the control, nonpathological animals (saline group).

### *Experimental groups*

After BLM instillation, animals were randomly divided further into four experimental groups as follows: BLM group: BLM-instilled rats that received no further treatments (n=10); CTRL group: saline-instilled rats (n=10); MSC group: BLM-instilled rats and adipose-derived MSC (n=10); and CM group: BLM-instilled rats and CM (n=10). Animals from each experimental group, including those from the saline group, were euthanized 21 days after BLM/saline instillation.

### *Treatment with MSC and CM*

Ten days after BLM instillation, a single dose of MSC ($1\times10^6$ cells in 0.2 mL of serum-free media) and concentrated CM (200 μL, derived from $1\times10^6$ cells) were injected into the caudal vein of each treated rat (Fig. 1A), as previously described by Cahill (Cruz et al., 2015; Cahill et al., 2016).

### *Clinical signs, mortality, and body weight*

Clinical signs and mortality were observed daily over the entire duration of the study. Body weights were measured just before instillation (day 0) and once a week (days 7, 14, and 21) post-BLM instillation and MSC/CM treatment.

### *Plasma inflammatory mediator levels*

At day 14 and 21 after BLM or saline instillation, rats were anesthetized and blood was drained from the abdominal aorta into a heparinized syringe and immediately used for analysis. Plasma was obtained, and fibrinogen, Von Willebrand factor, and PDGF were quantified by enzyme-linked immunosorbent assay, as previously described by our laboratory group (Sandrim et al., 2016).

### *Histologic evaluation of lung injury*

After euthanasia, lungs were extracted, fixed in buffered 10% formalin for 24 hours at room temperature (RT), and entirely sectioned. All sections from each individual rat were then embedded in a paraffin block. Consecutive 3-$\mu$m-thick sections of each sample were stained with hematoxylin and eosin for histological changes and with Verhöff-Masson trichrome for total collagen fibers. All histological analyses were performed in a blinded manner by two pathologists (A.T.F. and V.L.C.), as described below.

### *Immunohistochemistry evaluation of inflammatory and fibrotic mediators in lung tissue*

Lung sections were dewaxed in xylene, passed through a graded series of alcohols, and rehydrated in deionized water. Antigen retrieval was performed with a citrate buffer at pH 6.0 in a microwave oven for 15 min at 650 W, followed by an incubation of 20 min at RT. Endogenous peroxidases were blocked with the use of 0.5% hydrogen peroxide for 30 min, followed by three washes in 0.05% Tween Tris-buffered saline solution (TBST) at pH 7.6, unspecific labeling was reduced by 30 min of incubation at RT with normal serum (diluted 1:10 in TBST) from the same species from which the secondary antibodies were derived. After three washes, the sections were incubated overnight at 4°C with the following primary antibodies: anti-NOS-2 (Sc-651, 1:1000 dilution), anti-IL-17 (Sc-7927, dilution 1:100), anti-TGF-β1 (Sc-146, 1:500 dilution), anti-VEGF (SC-152, 1:100 dilution), and anti-endothelin-1 (Sc-21625, 1:100 dilution). After three washes, sections were incubated with an anti-rabbit or anti-rat horseradish peroxidase-conjugated secondary antibody (Vectastain, Vector Labs Inc, Cambridgeshire, UK) for 30 min at RT. Peroxidase reaction was developed for 10 min with the use of diaminobenzidine as the chromogen (Impact DAB, Vector Labs Inc) and blocked with deionized water. Substitution of the primary antibody with a rabbit- or rat-unrelated primary polyclonal serum served as a negative control.

Immunostained cells were quantified by histomorphometry. To access uniform and proportional lung samples, 10 fields (five nonoverlapping fields in two different sections) were randomly analyzed in proximal and distal lung parenchyma. The measurements were done with a 100-point and 50 straight grid with a known area ($10^3$ $\mu m^2$ at a 400× magnification) attached to the ocular of the microscope (Gundersen et al., 1988; Weibel, 2017). At 400× magnification, the number of positive immunostained cells in each field was calculated according to the number of points hitting positive cells for specific antibody as a proportion of the total grid area. Bronchi and blood vessels were carefully avoided during the measurements. To normalize the data, the number of positive cells, measured in each field, was divided by the length of each septum studied (to avoid any bias secondary to septal edema, alveolar collapse, and denser tissue matrix seen in the fibrotic sections). The results were expressed as the number of positive cells/$mm^2$ of connective tissue.

### *Immunofluorescence evaluation for collagen fibers*

To identify collagen fibers type I and V, we employed immunofluorescence. Antibodies were prepared as previously described (Spiess et al., 2007). Briefly, the sections of all groups were washed in xylene and dehydrated in graded ethanol. Antigen retrieval was done by enzymatic treatment of lungs with bovine pepsin (10,000 UTD) (Sigma Chemical Co.) in 0.5N acetic acid buffer (pH=2.5; 4 mg/mL) for 30 min at 37°C, followed by incubation with 5% bovine serum albumin in PBS. The slides were then incubated overnight at 4°C with rabbit polyclonal antibody anti-collagen type I (1:100, Rockland, Limerick, PA, USA) and rabbit polyclonal antihuman Col V (1:2000). For negative controls, sections were incubated with fetal bovine serum instead of the primary antibody. Finally, the sections were incubated with a goat anti-rabbit

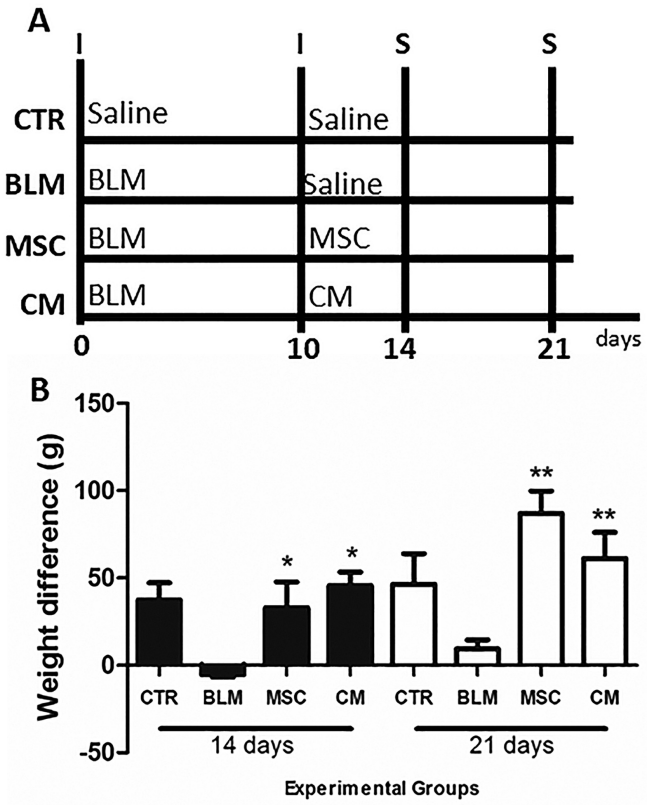


**Fig. 1.** Experimental Design and Weight difference. **A.** Note that the BLM instillation (I) is D0 and MSC/CM instillation is D10. Saline is used as control. **B.** The weight loss is height med greater in BLM group. Comparisons by Student's t test followed by Bonferroni's corrections for three comparisons. * $p<0.05$ vs BLM; ** $p<0.01$ vs BLM.

immunoglobulin ALEXA 488 (dilution 1:200; Invitrogen, Life Technologies, Thermo Fisher Scientific, Rockford, IL), diluted in PBS containing 0.0006% Evans Blue and mounted with 3-aminopropyltriethoxysilane.

Collagenous fibers (total, collagen type I and V) were quantified by optical density in the image analysis system (Image Pro-Plus 6.0) in 10 different, randomly selected alveolar septa, as previously described by our group (Parra et al., 2006). The results were expressed as the volume of collagen fibers/mm$^2$ of collagen tissue.

### *Statistical analysis*

Each variable was tested for normality and variance using the Kolmogorov-Smirnov and Levene tests, respectively. Data are presented as mean ± SD unless otherwise specified. On day 14, parametric data were compared by a one-sample Student's t test ($\alpha$<0.05). For comparisons between BLM at 14 days versus CTRL, BLM-MSC, and BLM-CM at 21 days, paired t tests were used ($\alpha$<0.05). On day 21, parametric and nonparametric data were analyzed by multiple Student t tests and Wilcoxon signed-rank tests, respectively, followed by Bonferroni's correction (adjusted $\alpha$*<0.0167 for four comparisons: CTRL vs BLM, CTRL vs BLM-MSC, CTRL vs BLM-CM, and CTRL vs BLM). The Bonferroni-adjusted significance level was used to counteract multiple comparisons. P<0.05 was adopted as significant. All tests were performed in SPSS software v.13.0 (SPSS, Inc., Chicago, IL, 2004).

## Results

### *Clinical signs, mortality, and body weight after BLM instillation and MSC and CM intravenous (IV) injection*

The BLM, BLM-MSC, and CM groups did not exhibit obvious clinical signs or mortality. Assessment of the effects of BLM, MSC, and CM IV injection on body weight revealed that after 14 days, as expected, rats from the BLM group showed a significant loss in body weight when compared with rats of the saline group (P<0.05; Fig. 1B). Rats that had been injected with MSC and CM showed a significant increase in weight and significant improvements at 14 and 21 days after IV injection that were very close to values shown by rats of the saline group at this same time point (P<0.05; Fig. 1B). Twenty-one days after BLM instillation, rats from the BLM group regained body weight. Rats of the BLM-MSC and CM groups progressively gained weight, which was higher than that of the BLM group and rats of the saline group at this same time point (Fig. 1B). In time, the rats of the BLM-MSC group regained body weight, albeit to a lesser extent than rats from the BLM-CM group (Fig. 1B).

### *BLM lung injury*

Twenty-one days after BLM instillation, lungs showed alveolar collapse and marked fibrotic areas (Fig. 2B) when compared with control (Fig. 2A) groups. The permanent alveolar damage caused a critical increase in total collagen deposition in small vessels and distal lung parenchyma in the BLM group (Figs. 3F, 4B; P<0.05) as compared with the CTRL group (Figs. 3F, 4A). In BLM lungs of the CTRL group, collagen I fibers were loosely arranged around bronchiole and vessels and along the alveolar septa, assuming a uniform distribution and enhancing alveolar architecture (Fig. 4A). In contrast, on day 21 after BLM instillation, significantly thicker collagen I fibers were tightly packed around the bronchiole, vessels, and along the alveolar septa, modifying the usual histoarchitecture of alveoli when compared with control (Figs. 3D, 4F; P<0.05). Col V analysis in the CTRL group showed loose fibers in a homogeneous, linear distribution along the alveolar septa and around the vessels (Fig. 4I), consistent with normal lung architecture. In contrast, after 14 and 21 days, BLM exhibited a significant increase in thick Col V fibers assuming an irregular and micronodular distribution involving the alveolar septa and small vessels in the BLM groups when compared with control (Figs. 3E, 4J; P<0.05). Ultrastructurally, these fibers were increased and strongly disarranged and tended to accumulate around myofibroblasts (Fig. 4N), in contrast to the uniform distribution in control lungs (Fig. 4M). Compared with control, TGF-$\beta$ (Figs. 2G, 3G), NOS (Figs. 2H, 3K), IL-17 (Figs. 2O, 3I), endothelin (Figs. 2S, 3J), and VEGF (Figs. 2X, 3K) immunophenotypes were significantly overexpressed in BLM at 14 and 21 days (P<0.05), respectively. At 14 days, BLM rats also showed significantly decreased levels of plasma fibrinogen (Fig. 3A), whereas BLM rats at 21 days presented increased plasma levels of Von Willebrand factor (Fig. 3B) and PDGF (Fig. 3C) compared with the CTRL group (P<0.05, respectively). Univariate analysis demonstrated that the level of Col V in BLM lungs was directly related to IL-17 (R=0.89; p=0.03), whereas $NO_2$ expression was inversely associated with fibrinogen level (R=-0.81; p=0.02).

### *Effect of CM and MSC on lung injury*

After 14 days, IV delivery of CM and MSCs led to a similar reduction in lung fibrosis, total collagen (Figs. 2C,D, 3F), and collagen I fibers (Figs. 3D, 4G,H,O,P) compared with the BLM group (P<0.05). Actually, CM-injected animals exhibited amounts of lung collagen I fibers that were significantly lower at day 21 than the amount observed in rats from the BLM and MSC groups (Figs. 3D, 4G; P<0.05). In contrast, CM injection was able to significantly increase the deposition of Col V fibers both at day 14 and at day 21 as compared with the amount observed in rats from the BLM group and MSC groups (Figs. 3E, 4K; P<0.05). To gain some insights into the possible mechanism underlying the beneficial effects of CM and MSC, we analyzed the

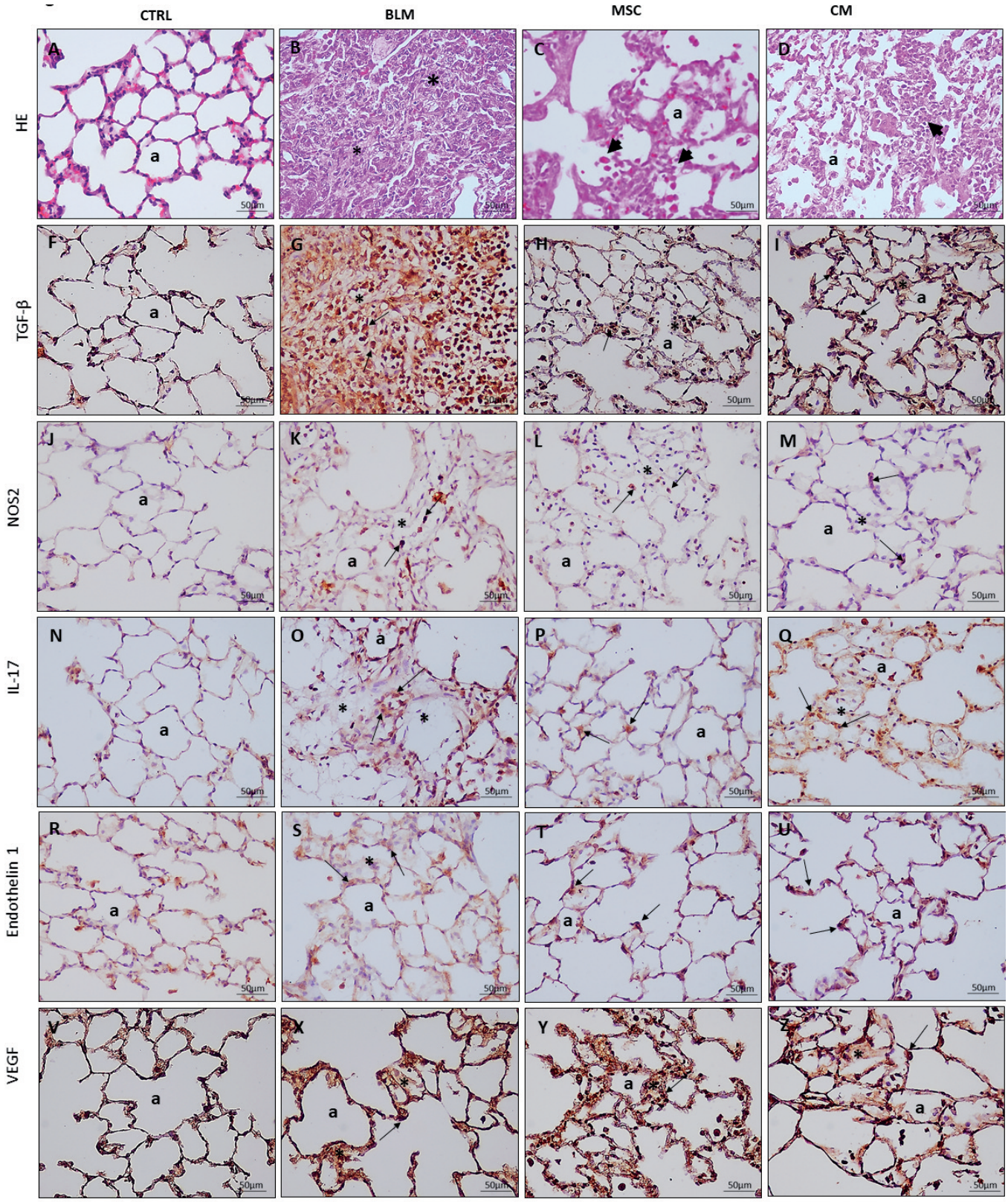


**Fig. 2.** Histological assessment and immunohistochemistry in lung tissue during the time course of BLM-induced lung fibrosis and BLM-CM and BLM-MSC treatment. **A-D, F-Z.** Representative light micrographs in lung tissue sections of saline and BLM-instilled mice and BLM-MSC and BLM-CM treatment stained with hematoxylin-eosin and immunohistochemistry, respectively. **A.** Saline-instilled rats. **B-D, F-Z.** BLM-instilled rats and BLM-MSC and BLM-CM at 21 days, respectively. **B.** Histopathology shows inflammation (arrows) and areas of lung fibrosis (*) with a more severe and diffused fibrotic reaction at 21 days allied to the distortion of pulmonary histoarchitecture. **C-D.** Attenuation of inflammation (arrows) and lung fibrosis (*) after BLM-MSC and BLM-CM treatment. **F-Z.** Lung parenchyma immunostained with TGB-β **(F-I)**, NOS2 **(J-M)**, IL-17 **(N-Q)**, endothelin **(R-U)** and VEGF **(V-Z)** antibodies. Note low expression of cytokines/chemokines in inflammatory (arrows) and endothelial (arrows) cells in rats of both experimental groups, with the exception of IL-17, which showed over expression in rats of CM and MSC groups with respect to animals of the BLM group. CTR, control, BLM, bleomycin, BLM-MSC, bleomycin-mesenchymal stromal cells, BLM-CM, bleomycin-conditioned medium, a, alveoli.

immunophenotypes of both proinflammatory mediators and profibrotic cytokines, which have been shown to be central to the pathogenesis of lung injury. Meanwhile, significantly lower expression of all of these mediators and cytokines was observed in rats of the CM and MSC groups when compared with rats of the BLM group ($P<0.05$): TGF-β (Figs. 2H,I, 3G), NOS2 (Figs. 2L,M, 3H), endothelin (Figs. 2T,U, 3J), and VEGF (Figs. 2Y,Z, 3K) immunophenotypes. At days 14 and 21, the levels of all cytokines/chemokines were low in rats of both experimental groups, with the exception of IL-17, which showed significantly higher expression in rats of the CM and MSC groups as compared with animals of the BLM group (Figs. 2P,O, 3I; $P<0.05$). Meanwhile, rats injected with CM and MSCs showed significant improvements at both time points of the analysis. At day 14, when compared with rats of the BLM group, these animals showed lower levels of plasma fibrinogen, PDGF, and Von Willebrand factor compared with the control group (Fig. 3A-C; $P<0.05$), the levels of which were all closer to those observed in the saline group. At day 21, mice of the CM and MSC groups maintained these parameters at levels similar to those recorded at day 14, which were significantly lower with respect to those observed in the BLM group.

## Discussion

In the present study, we investigated the beneficial effects of a cell-free treatment on the basis of the use of CM derived from cells isolated from the adipose mesenchymal tissue in rats with BLM-induced pulmonary fibrosis. First, we confirmed the CM's ability to maintain lung fibrosis at levels lower than those observed in untreated rats, and we extended the time of analysis to 21 days; furthermore, through comparative studies, we demonstrated the specificity of CM's action with respect to MSC derived from adipose tissue. Second, we showed that CM mediated improvement of immunomediators of inflammation and fibrosis. Finally, we provided insight into the possible key markers that may be responsible for the observed reduction in fibrosis.

In the current study, we decided to initiate MSC and

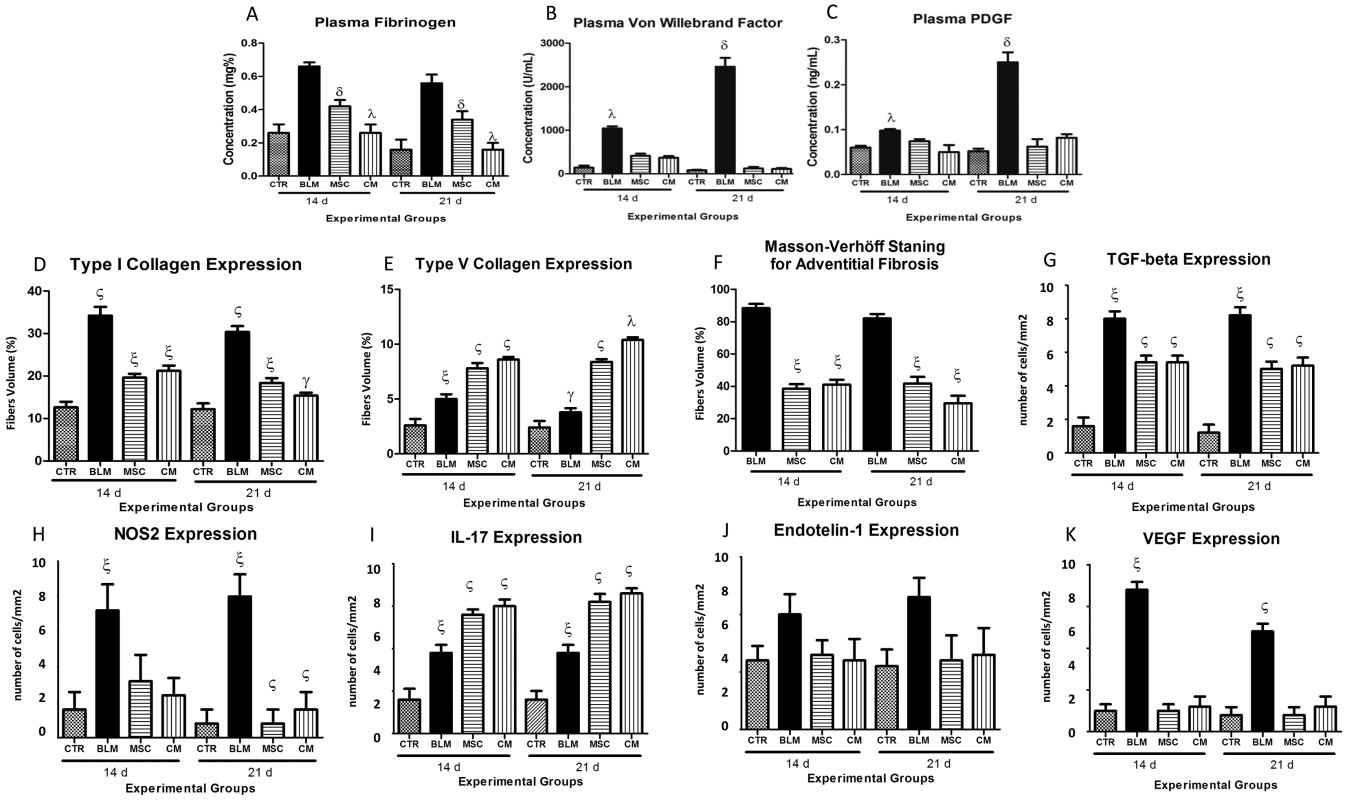


**Fig. 3.** Quantification of fibrinogen, Von Willebrand factor and PDGF of plasma levels, collagenous fibers and cytokines/interleukines density. Collagenous fibers were quantified by optical density at the image analysis system and expressed as the volume of collagen fibers/mm$^2$ of collagen tissue. Positive cytokines/interleukins cell density were determined by point-counting and expressed as the number of positive cells/mm$^2$ of connective tissue. Box represent means, and whiskers are the standard deviation of ten animals in each group. Comparisons by Student's t test followed by Bonferroni's corrections for four comparisons (*$p<0.0167$). CTR control, BLM bleomycin, BLM-MSC, bleomycin-mesenchymal stroma cells, BLM-CM, bleomycin-conditioned medium.

CM IV injection on day 10 with only a single injection, instead of repeated MSC administration, at 10 days, when BLM lung fibrosis has been established and presented features that resembled those with which clinicians typically deal. Timing and frequency of administration are very controversial in the literature and deserve some comments. Most studies administered MSCs within hours to a few days after BLM injury. Few studies administered MSCs at 7 (Gazdhar et al., 2013; Huang et al., 2015) or 10 (Moodley et al., 2013) days, and 1 study examined chronic lung injury with BLM injection twice weekly for 16 weeks and MSC administration at weeks 8, 10, 12, and 14 (Lee et al., 2014). In the study by Moodley et al. (2013), MSC therapy decreased lung collagen content significantly at 14 and 28 days after BLM injury (13 and 27 days after cell administration) but not after 7 days. In the study by Ortiz et al. (2003), the effect was significant when cells

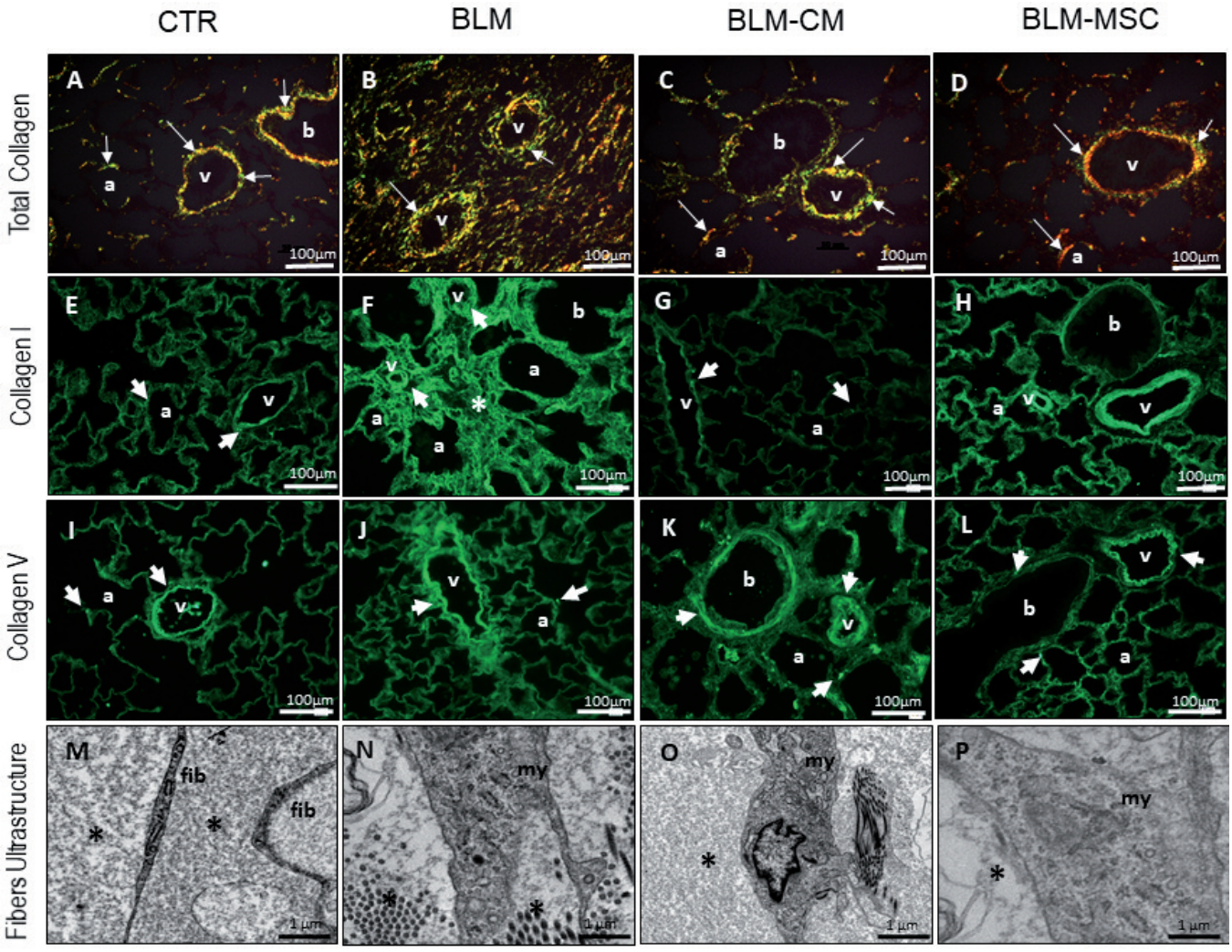


**Fig. 4.** Histochemical, immunofluorescence and electron microscopy assessment of total collagen, collagen I and V in lung tissue during the time course of BLM-induced lung fibrosis and MSC and CM injection. Representative micrographs in lung tissue sections of saline- and BLM-instilled rats stained with Picro-sirius and immunofluorescence counterstained with Blue Evans. **A, E, I, M.** Saline-instilled rats. **B, F, J, N.** BLM-instilled rats at 21 days, respectively. **A.** Picro-sirius shows weak yellow (long arrows) and green (short arrows) birefringence respectively of thick and thin fibers of total collagen in bronchiolar, alveolar and small vessels walls from the control groups. **E, I, M.** Immunofluorescence shows weak green birrefringence of Col I and Col V (arrow heads) in alveolar and small vessel walls coincident with uniform distribution of the fibers around fibroblasts at electron microscopy from the control groups. **B, F, J, N.** Pulmonary specimens of BLM 21 show diffuse increase of total collagen Col I and Col V green birefringence (arrow heads) in bronchiolar, alveolar and small vessels wall coincident with an increasead number and disarrangement of thick fibers around myofibroblasts at electron microscopy. **C, D, G, H, O.** Reduction of total collagen and collagen I fibers after CM and MSCs. **J, L.** Increase collagen V fiber deposition at day 21 after CM treatment. CTR control, BLM bleomycin, BLM-MSC, bleomycin-mesenchymal stroma cells, BLM-CM, bleomycin-conditioned medium. a, alveoli, b, bronchioles, fib, fibroblast, my, myofibroblast, *, collagen fibers, v, vessels, long arrows, collagen thick fibers, short arrows, collagen thin fibers, arrow heads, collagen I and V.

were given immediately but not when given 10 days after BLM administration. Lung collagen content was not decreased by repeated adipose tissue-derived MSC administration at 8, 10, 12, and 14 weeks in a chronic injury model in which BLM was given every 2 weeks for 16 weeks (Lee et al., 2014). Lung collagen assessed at 14 days was also not decreased by MSC administration twice, at 8 hours and 3 days after BLM injury, in the Aguilar et al. (2009) study. A systematic review of MSCs in an animal model of BLM pulmonary fibrosis done by Srour N and Thebaud B (2015) showed that administration of MSCs decreased lung collagen content and improved the Ashcroft score, bronchoalveolar lavage total cell count, neutrophil count, and lung TGF-β levels by day 10.

BLM-induced lung injury promotes alveolar cell damage and subsequent pulmonary inflammation and fibrosis because of its ability to produce oxygen radicals in the presence of iron and molecular oxygen (Sausville et al., 1978). Because CM and MSC were administered 10 days after induction of BLM injury, we first evaluated whether both treatments could influence the lung's inflammatory response to BLM-induced alveolar epithelial damage, reducing inflammation and subsequent fibrosis. Although this matter is controversial, some studies support a pivotal role of inflammation in fibrosis development (Wynn, 2011; Todd et al., 2012). Therefore, to confirm the early stage of BLM-induced lung injury, we evaluated weight loss, a marker of inflammatory status; fibrinogen, a classical positive acute-phase reactant protein; and NOS-2, a critical enzyme to the development of the acute inflammatory response to injury and necessary to control the late-phase response (Lee et al., 2010). In fact, we found that the weight loss was very expressive and the dosage of fibrinogen in plasma reduced in the BLM group coincided with *in situ* overexpression of NOS-2 immunophenotype. In contrast, rats that had been treated with MSCs and CM at 14 days after treatment showed a significant increase in weight, possibly related to lung fibrosis recovery. Although we used fetal bovine serum free, it is also possible that the gain in body weight was a consequence of growth factors in serum present in both MSCs and CM. Fibrinogen concentrations decreased from 0.7 mg/% after BLM to 0.3 and 0.2 mg/% at 2 weeks after MSCs and CM injection, after which they gradually decreased toward normal levels. This pattern of fibrinogen alteration correlated well with the inflammatory phase of the BLM response. Plasma fibrinogen may thus represent a rapid and sensitive marker of the acute phase response in the rat. In addition, lung content of NOS-2 mediators was found in the MSC and CM groups, which triggers the inflammatory response in BLM-induced lung injury, therefore supporting an early anti-inflammatory action of MSC and CM. Since these mediators are also responsible for initiation of the fibrotic process by modulating the expression of TGF-β, the early anti-inflammatory action of MSCs and CM may also explain the reduced TGF-β immunophenotype, lung fibrosis, total collagen, and collagen I fibers that we found in animals of both of these groups compared with rats of the other groups. These findings also coincide with improvements at both time points of analysis of plasma fibrinogen, PDGF, and Von Willebrand factor in treated animals compared with the saline group. Von Willebrand Factor and endothelin are important markers of endothelial activation and injury. Ware et al. (2004) reported that plasma levels of Von Willebrand factor, a marker of endothelial activation and injury, would be associated with clinical outcomes in acute lung injury. They found that baseline Von Willebrand factor levels were similar in patients with and without sepsis and were significantly higher in nonsurvivors as compared with survivors, even when controlling for severity of illness, sepsis, and ventilator strategy. Higher levels of Von Willebrand factor were also significantly associated with fewer organ failure-free days. They concluded that the degree of endothelial activation and injury is strongly associated with outcomes in acute lung injury/acute respiratory distress syndrome, regardless of the presence or absence of sepsis, and is not modulated by a protective ventilatory strategy. To improve outcomes further, new treatment strategies targeted at the endothelium should be investigated.

In the present study, CM and MSCs seemed to differentially modulate the production of some chemokines and growth factors associated with the pathophysiology of lung fibrosis. Increasing evidence demonstrates that the pathogenic changes mediated by MSCs are highly sensitive to the microenvironment to which these cells are exposed. For example, MSC-CMs may be a rich source of TGF-β secretion and lead to an increase in collagen gene expression (Salazar et al., 2009). Conversely, in an experimental model of BLM-induced fibrosis, adipose MSCs reduced lung tissue TGF-β levels and soluble collagen in lung extracts (Lee et al., 2010). In our study, a similar reduction of TGF-β expression and collagen I was observed in CM- and MSC-treated groups; however, it was not accompanied by an equal decrease in IL-17 and deposition of Col V fibers in the small vessels and lung parenchyma.

We found that CM treatment was able to significantly increase the deposition of Col V fibers both at day 14 and at day 21 as compared with the amount observed in rats from the BLM group and MSC group. Col V has been implicated in the regulation of *in vivo* adipose tissue growth (Minchin et al., 2015). Col V is expressed by preadipocytes (Hocking et al., 2010) and has a stimulatory effect on adipocyte hyperplasia (Nakajima et al., 2002b). Indeed, adipocyte differentiation is characterized by increased Col V accumulation, followed by a decline in Col V as adipose maturation proceeds (Nakajima et al., 2002a). Minchin and colleagues (Minchin et al., 2015) using *in vivo* imaging and genetic analysis in zebrafish showed that Col V is associated with "hyperplastic" adipose conditions and speculated that increased Col V may be

selectively induced and beneficial in situations in which hyperplastic growth is needed, such as insulin-resistant adipose tissue in obese and diabetic persons. Previous reports demonstrated the ability of MSCs to decrease VEGF expression *in vivo* (Lee et al., 2010; de Mendonca et al., 2017) in experimental models of lung injury/fibrosis. Actually, we observed that IV administration of MSCs and CM decreased VEGF and endothelin activation in lung tissue, suggesting protective and regenerative effects on pulmonary vascular endothelial cells, reducing the number of capillaries, and reducing vascular permeability as previously reported by Zhao and colleagues (Zhao et al., 2005). During recovery, VEGF may also take part in angiogenesis, an important component of lung repair (Zhao et al., 2005). Interestingly, Minchin and colleagues (Minchin et al., 2015) demonstrated that Col V induction in PLXND1 mutants is localized to vascular endothelial cells, suggesting that blood vessels are the source of adipose tissue morphology. Yang and colleagues (Yang et al., 2018) investigated *in vitro* the effects of human bone marrow-derived MSCs in the necrotic area of patients with steroid-induced necrosis of the femoral head. They found that the immunoexpression of Col V and VEGF was significantly decreased after treatment of necrosis of the femoral head.

In the current study, the abnormal and disrupted Col V bundles described also support the concept that exposure of immunogenic epitopes as previously reported in fibrotic lung diseases (Parra et al., 2006, 2009; Souza et al., 2010; Tiriveedhi et al., 2012) may trigger a Th17-dependent immune response (Burlingham et al., 2007; Khoury, 2011). Interestingly, we demonstrated that the levels of all cytokines/chemokines were low in rats of both experimental groups, with the exception of IL-17, which showed expression that was significantly higher in rats of the CM and MSC groups with respect to animals of the BLM group. We also found increased Col V in rat lungs after CM and MSC treatment, which might appear to be contradictory in the pathogenesis of fibrosis, when it is argued that raising the level of Col V is beneficial in lung fibrosis. At this point, it is important to remember that we found a significant decrease in Col I in rats of the CM and MSC groups. As previously demonstrated, a positive feedback loop between the Col V and IL-17 expression patterns harmonizes the maintenance of Col I in the late stage of BLM model recovering the lung fibrosis (Parra et al., 2006; Wilson et al., 2010; Fabro et al., 2015). Taken together, these findings suggest a positive feedback triggered by cell treatment among Col V, Th17 response, and non-myofibroblastic activation. In this situation, an imbalance between decreased collagen I and increased Col V favors a Col V-mediated IL-17 immune response, resulting in blockade of myofibroblast activation by a decrease in deposition of collagen I fibers after recovery of lung fibrosis. The exact mechanism of IL-17 immune modulation by MSCs or their paracrine effect is not yet known in pulmonary fibrosis. Other studies should be carried out to investigate whether regulation of Th17 and IL-17 may be intimately involved in this process.

In the current study, we found better beneficial effects of CM derived from cells isolated from the adipose mesenchymal tissue, indicating that immunomodulatory properties of adipose-derived MSC CMs are more effective than direct intercellular communications of MSC, as previously reported (Linero and Chaparro, 2014; Li et al., 2015). Interestingly, Cargnoni and colleagues (Cargnoni et al., 2014) reported robust evidence favoring such a mechanism by administering CM derived from the culture of cells isolated from the adipose tissue (MSC) to BLM-injured mice, rather than administering the cells themselves. These authors found that even in the absence of cells, mice treated with CM developed less accentuated lung fibrosis, fibroblast proliferation, collagen deposition, and alveolar obliteration when compared with untreated mice. In fact, we found that ultrastructural features of myofibroblastic activation, including fibronexus, rough endoplasmic reticulum, and mitochondria, were less prominent in lungs from CM animals compared with MSC and BLM, supporting the positive therapeutic effects of CM as previously reported in the literature (Hinz et al., 2007; Eyden, 2008). However, CM presents disadvantages, such as culture conditions, that are detrimental for cell transplantation and risk of contamination and immunologic reactions. Based on these limitations, some investigators prefer MSCs, which can be easily and safely administered on the day of harvesting, can express several genes involved in inflammatory response and chemotaxis, and can present lower cost (Ohnishi et al., 2007; Araujo et al., 2010).

Several limitations of this study should be considered: (1) there is an absence of *in vitro* work for gene expression and protein analysis; (2) MSC was tracked after IV administration, limiting our knowledge regarding the delivery dynamics of cell lineage; (3) the experimental period was 21 days, which may not be enough to understand the late effects of MSC and CM therapy; (4) only a few specific cytokines and growth factors were evaluated, and a wider range of mediators should be analyzed to provide a more complete understanding of the mechanisms associated with each cell treatment; and 5) we did not show the effect of adipose-derived MSCs and their CM on anti-Col V reactive T-cell levels. In addition, more extensive analysis of the range of soluble mediators released by MSCs and CM may provide further information on the different effects noted in this model.

In summary, this study reinforces previous observations on the therapeutic properties of MSCs and CM and is the first report to demonstrate the association of their actions with immunomodulatory biomarkers on lung tissue. We concluded that adipose-derived stem cells and adipose-derived stem cells-CM modulate the *in situ* imbalance between the collagen I- and Col V-mediated IL-17 immune response, emerging as a

promising therapeutic option for recovering from BLM pulmonary fibrosis.

*Acknowledgements.* The authors are grateful to Paulo Cesar Georgete and Luiz Carlos Edevalter Bardella for excellent technical support in UNIPEX/UNESP, and Sandra de Morais Fernezlian and Esmeralda Ministene Eher for their help with immunohistochemistry in FMUSP. The authors also are grateful for the financial support provided by the National Council for Scientific and Technological Development [CNPq-471939/2010-2 and 483005/2012-6]; Foundation for the Support of Research of the State of São Paulo [FAPESP 12/03543-2, FAPESP11/09181-2, FAPESP 2012/07040-5, FAPESP 2013/05886-7, FAPESP 2013/14277-4, FAPESP 2018/20403-6]; and the Laboratories for Medical Research [LIMs], Hospital das Clinicas, University of São Paulo. and Coordination for the Improvement of Higher Level Personnel (CAPES).

## References

Aguilar S., Scotton C.J., McNulty K., Nye E., Stamp G., Laurent G., Bonnet D. and Janes S.M. (2009). Bone marrow stem cells expressing keratinocyte growth factor via an inducible lentivirus protects against bleomycin-induced pulmonary fibrosis. PLoS One 4, e8013.

Araujo I.M., Abreu S.C., Maron-Gutierrez T., Cruz F., Fujisaki L., Carreira H. Jr, Ornellas F., Ornellas D., Vieira-de-Abreu A., Castro-Faria-Neto H.C., Muxfeldt Ab'Saber A., Teodoro W.R., Diaz B.L., Peres Dacosta C., Capelozzi V.L., Pelosi P., Morales M.M. and Rocco P.R. (2010). Bone marrow-derived mononuclear cell therapy in experimental pulmonary and extrapulmonary acute lung injury. Crit. Care Med. 38, 1733-1741.

Axtell R.C., de Jong B.A., Boniface K., van der Voort L.F., Bhat R., De Sarno P., Naves R., Han M., Zhong F., Castellanos J.G., Mair R., Christakos A., Kolkowitz I., Katz L., Killestein J., Polman C.H., de Waal Malefyt R., Steinman L. and Raman C. (2010). T helper type 1 and 17 cells determine efficacy of interferon-beta in multiple sclerosis and experimental encephalomyelitis. Nat. Med. 16, 406-412.

Bateman M.E., Strong A.L., Gimble J.M. and Bunnell B.A. (2018). Concise review: Using fat to fight disease: A systematic review of nonhomologous adipose-derived stromal/stem cell therapies. Stem Cells 36, 1311-1328.

Bertanha M., Moroz A., Almeida R., Alves F.C., Acorci Valerio M.J., Moura R., Domingues M.A., Sobreira M.L. and Deffune E. (2014). Tissue-engineered blood vessel substitute by reconstruction of endothelium using mesenchymal stem cells induced by platelet growth factors. J. Vasc. Surg. 59, 1677-1685.

Burlingham W.J., Love R.B., Jankowska-Gan E., Haynes L.D., Xu Q., Bobadilla J.L., Meyer K.C., Hayney M.S., Braun R.K., Greenspan D.S., Gopalakrishnan B., Cai J., Brand D.D., Yoshida S., Cummings O.W. and Wilkes D.S. (2007). Il-17-dependent cellular immunity to collagen type v predisposes to obliterative bronchiolitis in human lung transplants. J. Clin. Invest. 117, 3498-3506.

Cahill E.F., Kennelly H., Carty F., Mahon B.P. and English K. (2016). Hepatocyte growth factor is required for mesenchymal stromal cell protection against bleomycin-induced pulmonary fibrosis. Stem Cells Transl Med. 5, 1307-1318.

Cargnoni A., Piccinelli E.C., Ressel L., Rossi D., Magatti M., Toschi I., Cesari V., Albertini M., Mazzola S. and Parolini O. (2014). Conditioned medium from amniotic membrane-derived cells prevents lung fibrosis and preserves blood gas exchanges in bleomycin-injured mice-specificity of the effects and insights into possible mechanisms. Cytotherapy 16, 17-32.

Cruz F.F., Borg Z.D., Goodwin M., Sokocevic D., Wagner D.E., Coffey A., Antunes M., Robinson K.L., Mitsialis S.A., Kourembanas S., Thane K., Hoffman A.M., McKenna D.H., Rocco P.R., Weiss D.J. (2015). Systemic administration of human bone marrow-derived mesenchymal stromal cell extracellular vesicles ameliorates *Aspergillus hyphal* extract-induced allergic airway inflammation in immunocompetent mice. Stem Cells Transl. Med. 4, 1302-1316.

de Mattos Carvalho A., Alves A.L., Golim M.A., Moroz A., Hussni C.A., de Oliveira P.G. and Deffune E. (2009). Isolation and immunophenotypic characterization of mesenchymal stem cells derived from equine species adipose tissue. Vet. Immunol. Immunopathol. 132, 303-306.

de Mendonca L., Felix N.S., Blanco N.G., Da Silva J.S., Ferreira T.P., Abreu S.C., Cruz F.F., Rocha N., Silva P.M., Martins V., Capelozzi V.L., Zapata-Sudo G., Rocco P.R.M. and Silva P.L. (2017). Mesenchymal stromal cell therapy reduces lung inflammation and vascular remodeling and improves hemodynamics in experimental pulmonary arterial hypertension. Stem Cell Res. Ther. 8, 220.

Eyden B. (2008). The myofibroblast: Phenotypic characterization as a prerequisite to understanding its functions in translational medicine. J. Cell Mol. Med. 12, 22-37.

Fabro A.T., da Silva P.H., Zocolaro W.S., de Almeida M.S., Rangel M.P., de Oliveira C.C., Minatel I.O., Prando E.D., Rainho C.A., Teodoro W.R., Velosa A.P., Saber A.M., Parra-Cuentas E.R., Popper H.H. and Capelozzi V.L. (2015). The Th17 pathway in the peripheral lung microenvironment interacts with expression of collagen V in the late state of experimental pulmonary fibrosis. Immunobiology 220, 124-135.

Gazdhar A., Susuri N., Hostettler K., Gugger M., Knudsen L., Roth M., Ochs M. and Geiser T. (2013). HGF expressing stem cells in usual interstitial pneumonia originate from the bone marrow and are antifibrotic. PLoS One 8, e65453.

Gerdoni E., Gallo B., Casazza S., Musio S., Bonanni I., Pedemonte E., Mantegazza R., Frassoni F., Mancardi G., Pedotti R. and Uccelli A. (2007). Mesenchymal stem cells effectively modulate pathogenic immune response in experimental autoimmune encephalomyelitis. Ann. Neurol. 61, 219-227.

Gundersen H.J., Bendtsen T.F., Korbo L., Marcussen N., Moller A., Nielsen K., Nyengaard J.R., Pakkenberg B., Sorensen F.B., Vesterby A. and West M.J. (1988). Some new, simple and efficient stereological methods and their use in pathological research and diagnosis. APMIS. 96, 379-394.

Hinz B., Phan S.H., Thannickal V.J., Galli A., Bochaton-Piallat M.L. and Gabbiani G. (2007). The myofibroblast: One function, multiple origins. Am. J. Pathol. 170, 1807-1816.

Hocking S.L., Wu L.E., Guilhaus M., Chisholm D.J. and James D.E. (2010). Intrinsic depot-specific differences in the secretome of adipose tissue, preadipocytes, and adipose tissue-derived microvascular endothelial cells. Diabetes 59, 3008-3016.

Huang K., Kang X., Wang X., Wu S., Xiao J., Li Z., Wu X. and Zhang W. (2015). Conversion of bone marrow mesenchymal stem cells into type II alveolar epithelial cells reduces pulmonary fibrosis by decreasing oxidative stress in rats. Mol. Med. Rep.11, 1685-92.

Ionescu L., Byrne R.N., van Haaften T., Vadivel A., Alphonse R.S., Rey-

Parra G.J., Weissmann G., Hall A., Eaton F. and Thébaud B. (2012a). Stem cell conditioned medium improves acute lung injury in mice: *In vivo* evidence for stem cell paracrine action. Am. J. Physiol. Lung Cell Mol. Physiol. 303, L967-L977.

Ionescu L.I., Alphonse R.S., Arizmendi N., Morgan B., Abel M., Eaton F., Duszyk M., Vliagoftis H., Aprahamian T.R., Walsh K., and Thébaud B. (2012b). Airway delivery of soluble factors from plastic-adherent bone marrow cells prevents murine asthma. Am. J. Respir. Cell Mol. Biol. 46, 207-16.

Khoury S.J. (2011). Th17 and Treg balance in systemic sclerosis. Clin. Immunol. 139, 231-232.

Kilkenny C., Browne W.J., Cuthill I.C., Emerson M. and Altman D.G. (2010). Improving bioscience research reporting: The arrive guidelines for reporting animal research. J. Pharmacol. Pharmacother. 1, 94-99.

Kim S.N., Lee J., Yang H.S., Cho J.W., Kwon S., Kim Y.B., Her J.D., Cho K.H., Song C.W. and Lee K. (2010). Dose-response effects of bleomycin on inflammation and pulmonary fibrosis in mice. Toxicol. Res. 26, 217-212

Lee S.H., Jang A.S., Kim Y.E., Cha J.Y., Kim T.H., Jung S., Park S.K., Lee Y.K., Won J.H., Kim Y.H. and Park C.S. (2010). Modulation of cytokine and nitric oxide by mesenchymal stem cell transfer in lung injury/fibrosis. Respir. Res. 11, 16.

Lee S.H., Lee E.J., Lee S.Y., Kim J.H., Shim J.J., Shin C., In K.H., Kang K.H., Uhm C.S., Kim H.K., Yang K.S., Park S., Kim H.S., Kim Y.M. and Yoo T.J. (2014). The effect of adipose stem cell therapy on pulmonary fibrosis induced by repetitive intratracheal bleomycin in mice. Exp. Lung Res. 40, 117-125.

Lei G.S., Kline H.L., Lee C.H., Wilkes D.S. and Zhang C. (2016). Regulation of collagen v expression and epithelial-mesenchymal transition by mir-185 and mir-186 during idiopathic pulmonary fibrosis. Am. J. Pathol. 186, 2310-2316.

Li X., Zhao H., Qi C., Zeng Y., Xu F. and Du Y. (2015). Direct intercellular communications dominate the interaction between adipose-derived MSCs and myofibroblasts against cardiac fibrosis. Protein Cell. 6, 735-745.

Linero I. and Chaparro O. (2014). Paracrine effect of mesenchymal stem cells derived from human adipose tissue in bone regeneration. PLoS One 9, e107001.

Mangan P.R., Harrington L.E., O'Quinn D.B., Helms W.S., Bullard D.C., Elson C.O., Hatton R.D., Wahl S.M., Schoeb T.R. and Weaver C.T. (2006). Transforming growth factor-beta induces development of the T(h)17 lineage. Nature 441, 231-234.

Mariman E.C. and Wang P. (2010). Adipocyte extracellular matrix composition, dynamics and role in obesity. Cell Mol. Life Sci. 67, 1277-1292.

Mi S., Li Z., Yang H.Z., Liu H., Wang J.P., Ma Y.G., Wang X.X., Liu H.Z., Sun W. and Hu Z.W. (2011). Blocking IL-17a promotes the resolution of pulmonary inflammation and fibrosis via TGF-beta1-dependent and -independent mechanisms. J. Immunol. 187, 3003-3014.

Minchin J.E., Dahlman I., Harvey C.J., Mejhert N., Singh M.K., Epstein J.A., Arner P., Torres-Vazquez J. and Rawls J.F. (2015). Plexin D1 determines body fat distribution by regulating the type V collagen microenvironment in visceral adipose tissue. Proc. Natl. Acad. Sci. USA 112, 4363-4368.

Moodley Y., Vaghjiani V., Chan J., Baltic S., Ryan M., Tchongue J., Samuel C.S., Murthi P., Parolini O. and Manuelpillai U. (2013). Anti-inflammatory effects of adult stem cells in sustained lung injury: a comparative study. PLoS One 8, e69299.

Moroz A., Bittencourt R.A., Almeida R.P., Felisbino S.L. and Deffune E. (2013). Platelet lysate 3D scaffold supports mesenchymal stem cell chondrogenesis: An improved approach in cartilage tissue engineering. Platelets 24, 219-225.

Murphy S., Lim R., Dickinson H., Acharya R., Rosli S., Jenkin G. and Wallace E. (2011). Human amnion epithelial cells prevent bleomycin-induced lung injury and preserve lung function. Cell Transplant. 20, 909-923.

Nakajima I., Muroya S., Tanabe R. and Chikuni K. (2002a). Extracellular matrix development during differentiation into adipocytes with a unique increase in type V and VI collagen. Biol. Cell 94, 197-203.

Nakajima I., Muroya S., Tanabe R. and Chikuni K. (2002b). Positive effect of collagen V and VI on triglyceride accumulation during differentiation in cultures of bovine intramuscular adipocytes. Differentiation 70, 84-91.

Nakano K., Yamaoka K., Hanami K., Saito K., Sasaguri Y., Yanagihara N., Tanaka S., Katsuki I., Matsushita S. and Tanaka Y. (2011). Dopamine induces IL-6-dependent IL-17 production via D1-like receptor on CD4 naive T cells and D1-like receptor antagonist sch-23390 inhibits cartilage destruction in a human rheumatoid arthritis/scid mouse chimera model. J. Immunol. 186, 3745-3752.

Ohnishi S., Yasuda T., Kitamura S. and Nagaya N. (2007). Effect of hypoxia on gene expression of bone marrow-derived mesenchymal stem cells and mononuclear cells. Stem Cells 25, 1166-1177.

Ortiz L.A., Gambelli F., McBride C., Gaupp D., Baddoo M., Kaminski N., Phinney D.G. Mesenchymal stem cell engraftment in lung is enhanced in response to bleomycin exposure and ameliorates its fibrotic effects. (2003). Proc. Natl. Acad. Sci. USA 100, 8407-8401.

Parra E.R., Teodoro W.R., Velosa A.P., de Oliveira C.C., Yoshinari N.H. and Capelozzi V.L. (2006). Interstitial and vascular type V collagen morphologic disorganization in usual interstitial pneumonia. J. Histochem. Cytochem. 54, 1315-1325.

Parra E.R., Aguiar A.C. Jr, Teodoro W.R., de Souza R., Yoshinari N.H. and Capelozzi V.L. (2009). Collagen V and vascular injury promote lung architectural changes in systemic sclerosis. Clin. Respir. J. 3, 135-142.

Reddy M., Fonseca L., Gowda S., Chougule B., Hari A. and Totey S. (2016). Human adipose-derived mesenchymal stem cells attenuate early stage of bleomycin induced pulmonary fibrosis: Comparison with pirfenidone. Int. J. Stem Cells 9, 192-206.

Salazar K.D., Lankford S.M. and Brody A.R. (2009). Mesenchymal stem cells produce Wnt isoforms and TGF-beta1 that mediate proliferation and procollagen expression by lung fibroblasts. Am. J. Physiol. Lung Cell Mol. Physiol. 297, L1002-1011.

Sandrim V.C., Dias M.C., Bovolato A.L., Tanus-Santos J.E., Deffune E. and Cavalli R.C. (2016). Plasma from pre-eclamptic patients induces the expression of the anti-angiogenic mir-195-5p in endothelial cells. J. Cell Mol. Med. 20, 1198-1200.

Sausville E.A., Peisach J. and Horwitz S.B. (1978). Effect of chelating agents and metal ions on the degradation of DNA by bleomycin. Biochemistry 17, 2740-2746.

Shi Y., Hu G., Su J., Li W., Chen Q., Shou P., Xu C., Chen X., Huang Y., Zhu Z., Huang X., Han X., Xie N. and Ren G. (2010). Mesenchymal stem cells: A new strategy for immunosuppression and tissue repair. Cell Res. 20, 510-518.

Spiess K., Teodoro W.R. and Zorn T.M.T. (2007). Distribution of collagen types I, III and V in pregnant mouse endometrium. Connect. Tissue Res. 48, 99-108.

Souza P., Rizzardi F., Noleto G., Atanazio M., Bianchi O., Parra E.R., Teodoro W.R., Carrasco S., Velosa A.P., Fernezlian S., Ab'saber A.M., Antonangelo L., Takagaki T., Schainberg C.G., Yoshinari N.H. and Capelozzi V.L. (2010). Refractory remodeling of the microenvironment by abnormal type V collagen, apoptosis, and immune response in non-small cell lung cancer. Hum. Pathol. 41, 239-248.

Srour N. and Thebaud B. (2015). Mesenchymal stromal cells in animal bleomycin pulmonary fibrosis models: A systematic review. Stem Cells Transl. Med. 4, 1500-1510.

Sun M., Chen S., Adams S.M., Florer J.B., Liu H., Kao W.W., Wenstrup R.J. and Birk D.E. (2011). Collagen V is a dominant regulator of collagen fibrillogenesis: Dysfunctional regulation of structure and function in a corneal-stroma-specific Col5a1-null mouse model. J. Cell Sci. 124, 4096-4105.

Tiriveedhi V., Angaswamy N., Brand D., Weber J., Gelman A.G., Hachem R., Trulock E.P., Meyers B., Patterson G. and Mohanakumar T. (2012). A shift in the collagen V antigenic epitope leads to T helper phenotype switch and immune response to self-antigen leading to chronic lung allograft rejection. Clin. Exp. Immunol. 167, 158-168.

Todd N.W., Luzina I.G. and Atamas S.P. (2012). Molecular and cellular mechanisms of pulmonary fibrosis. Fibrogenesis Tissue Repair 5, 11.

Vittal R., Fan L., Greenspan D.S., Mickler E.A., Gopalakrishnan B., Gu H., Benson H.L., Zhang C., Burlingham W., Cummings O.W. and Wilkes D.S. (2013a). IL-17 induces type V collagen overexpression and EMT via TGF-beta-dependent pathways in obliterative bronchiolitis. Am. J. Physiol. Lung Cell Mol. Physiol. 304, L401-414.

Vittal R., Mickler E.A., Fisher A.J., Zhang C., Rothhaar K., Gu H., Brown K.M., Emtiazdjoo A., Lott J.M., Frye S.B., Smith G.N., Sandusky G.E., Cummings O.W. and Wilkes D.S. (2013b). Type V collagen induced tolerance suppresses collagen deposition, TGF-beta and associated transcripts in pulmonary fibrosis. PLoS One 8, e76451.

Ware L.B., Eisner M.D., Thompson B.T., Parsons P.E. and Matthay M.A. (2004). Significance of von willebrand factor in septic and nonseptic patients with acute lung injury. Am. J. Respir. Crit. Care Med. 170, 766-772.

Weber D.J. and Wilkes D.S. (2013). The role of autoimmunity in obliterative bronchiolitis after lung transplantation. Physiol. Lung Cell Mol. Physiol. 304, L307-311.

Weibel E.R. (2017). Lung morphometry: The link between structure and function. Cell Tissue Res. 367, 413-426.

Weiss D.J., Bertoncello I., Borok Z., Kim C., Panoskaltsis-Mortari A., Reynolds S., Rojas M., Stripp B., Warburton D. and Prockop D.J. (2011). Stem cells and cell therapies in lung biology and lung diseases. Proc. Am. Thorac. Soc. 8, 223-272.

Wenstrup R.J., Smith S.M., Florer J.B., Zhang G., Beason D.P., Seegmiller R.E., Soslowsky L.J. and Birk D.E. (2011). Regulation of collagen fibril nucleation and initial fibril assembly involves coordinate interactions with collagens V and XI in developing tendon. J. Biol. Chem. 286, 20455-20465.

Wilson M.S., Madala S.K., Ramalingam T.R., Gochuico B.R., Rosas I.O., Cheever A.W. and Wynn T.A. (2010). Bleomycin and IL-1beta-mediated pulmonary fibrosis is IL-17a dependent. J. Exp. Med. 207, 535-552.

Wynn T.A. (2011). Integrating mechanisms of pulmonary fibrosis. J. Exp. Med. 208, 1339-1350.

Yang F., Luo P., Ding H., Zhang C. and Zhu Z. (2018). Collagen type V a2 (col5a2) is decreased in steroid-induced necrosis of the femoral head. Am J. Transl. Res. 10, 2469-2479.

Zhao L., Wang K., Ferrara N. and Vu T.H. (2005). Vascular endothelial growth factor co-ordinates proper development of lung epithelium and vasculature. Mech. Dev. 122, 877-886.

Accepted July 18, 2019